ChemComm

Discrimination of Dicarboxylic Acids via Assembly-Induced Emission

Journal:	*ChemComm*
Manuscript ID	CC-COM-08-2018-006689.R1
Article Type:	Communication

SCHOLARONE™
Manuscripts

Please do not adjust margins

Journal Name

COMMUNICATION

Discrimination of Dicarboxylic Acids via Assembly-Induced Emission

Received 00th January 20xx,
Accepted 00th January 20xx

DOI: 10.1039/x0xx00000x

www.rsc.org/

Zhenglin Zhang, Mohamed I. Hashim, Chia-Hua Wu, Judy I. Wu, and Ognjen Š. Miljanić*

Dicarboxylic acids are important chemicals in human metabolism and various industries. Differentiating among their isomers and members of homologous series is a challenge, due to their similar properties. We show that a triazine-based fluorinated AIEgen can recognize dicarboxylic acids with selectivity based on the relative position of the two –COOH groups.

Dicarboxylic acids and dicarboxylate anions are important chemicals in human metabolism.[1] Abnormal levels of dicarboxylic acids (fumaric, oxalic, malonic, and others) can indicate metabolic disorders, and the commercial tests for the physiological levels of dicarboxylic acids are available, guiding the corresponding clinical treatments.[2,3] In addition to their physiological significance, dicarboxylic acids also play important roles as food additives and preservatives (malic, fumaric, tartaric acids),[4] pharmaceutical formulations (oxalic, malonic, maleic acids),[5] precursors in polymer industry (succinic, terephthalic, adipic acids),[6] and intermediates in atmospheric studies (oxalic acid).[7] Therefore, the recognition of dicarboxylic acids and dicarboxylate anions is an important field of study.[8]

However, discrimination between dicarboxylic acids remains a challenge, as the recognition of isomers and members of homologous series becomes complicated by the similarities in the physical (high polarity) and chemical (dissociation and acidity) properties of these acids. A common strategy in molecular recognition is to design a preorganized binding cavity in a host molecule, which geometrically matches the size and noncovalent binding preferences of the guest.[9] For the recognition of dicarboxylic acids, a typical host has two or more binding sites, which are connected by a spacer and interact with dicarboxylic acids by intermolecular hydrogen bonds,[10] ionic bonding,[11] or hydrogen-π interactions.[12] The details of host and guest structures determine whether discrete complexes, infinite chains, or ribbon structure are formed.[10b,13] A host with a rigid cavity usually has a high selectivity for a targeted guest.[14] For example, Beer et al. recently reported that a [3]rotaxane with two macrocycles showed higher binding selectivity for (*S*)-glutamate vs. (*R*)-glutamate than that of the axle without the macrocycles, as the macrocycles formed a rigidified and preorganized cavity for the (*S*)-isomer.[15] Such highly selective hosts often require lengthy syntheses. More adjustable hosts can often accommodate several related guests, with different sizes but same functional groups.[16] If such adjustable hosts give off colorimetric or fluorescent signals,[8a,17] detectable by naked eye, their potential practical value can parallel that of highly specific hosts.

In this Communication, we present the use of a trigonal fluorinated trispyrazole **1** (Scheme 1) as the fluorophore which is selectively turned ON by the interaction with (*a*) *ortho*-isomers of aromatic dicarboxylic acids, (*b*) *cis*-isomers of alkene-based dicarboxylic acids, and (*c*) short-chain aliphatic α,ω-dicarboxylic acids. Diacids isomeric or homologous to these privileged analytes showed no fluorescence turn-ON.

Aggregation-induced emission (AIE) is observed when a solution of a non-luminescent solute (AIEgen) becomes luminescent as the aggregation of the AIEgen is triggered. This triggering is typically done by the addition of a second "bad" solvent, which is unable to dissolve the AIEgen.[18] The most common mechanism of AIE is the restriction of intramolecular motion (RIM), which causes the radiative decay of the excited state.[19] Consequently, any factors—and not only aggregation—which restrict intramolecular motions should

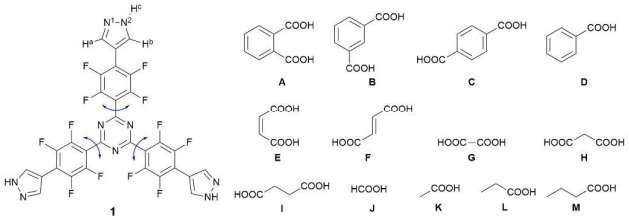

Scheme 1. The structures of compound **1** and the carboxylic acids tested in this paper.

University of Houston, Department of Chemistry,
112 Fleming Building, Houston, TX 77204-5003, USA.
E-mail: miljanic@uh.edu; Tel: + 1 832 842-8827.

Supporting information for this article is given via a link at the end of the document.

Please do not adjust margins

turn ON the luminescence of AIEgens. This notion is supported by the reports of complexes[20] and oligomers[21] in which AIEgens turned ON their luminescence without causing aggregation. Therefore, hosts with AIE properties may be a common "ruler" for guests of somewhat similar structures—isomers and members of homologous series—that can restrict their intramolecular motion to different degrees.

Recently, we have synthesized a series of rigid and extensively fluorinated aromatic compounds, which form porous solid-state structures through a combination of intermolecular hydrogen bonds and [π···π] stacking.[22] These porous molecular crystals showed fast adsorption of fluorinated compounds[23] and adsorbate-induced piezochromism.[24] Among the precursors to these porous structures, compound **1** has the lowest barriers to internal rotation (shown by arrows in Scheme 1)—on account of the absence of hydrogens on the central triazine ring—and exhibits AIE.[22b] The interactions between pyrazole and dicarboxylic acids[25] inspired us to study **1** as a potential sensor for dicarboxylic acids. We probed the fluorescent response of **1** to different aromatic (**A**–**D**, Scheme 1), alkene-based (**E** and **F**), and aliphatic (**G**–**M**) carboxylic acids. Most of the tested analytes were dicarboxylic acids, with monocarboxylic acids **D** and **J**–**M** also tested for comparison purposes. Dramatic differences were noticed in the response of **1** to these structurally related analytes.

The emission and absorption spectral responses of **1** to **A** were tested first (Figure 1 and Table S1). With the addition of **A** (up to 3 eq) into the solution of **1**, the relative integrated emission intensity (I/I_0) decreased to 0.68 with λ_{ems} shifting minimally—from 438 to 440 nm. With further addition of **A** (3–12 eq), however, the I/I_0 increased to 4.40 with a significant bathochromic shift of λ_{ems} to 490 nm and a visible turning ON of aquamarine fluorescence. With further addition of **A** (up to 48 eq), the fluorescence intensity decreased to I/I_0 = 1.5 with a hypochromic shift of λ_{ems} to 484 nm. The change in the emission intensity and λ_{ems} indicates that the excited state decay was influenced by the addition of **A**. For absorption spectra, the λ_{abs} = 323 nm was the characteristic peak of **1**, and it continued to appear at 323 or 324 nm after the addition of **A**, meaning that the conjugation system of **1** was hardly influenced by **A**. The peaks around 284 and 292 nm were the signals from **A**, and their intensity increased with the addition of **A**, as was expected. For classic AIE phenomena, the tails in the long wavelength side of the absorption spectra would level off as the scattering of nano-sized aggregates becomes more pronounced.[18,22b,26] However, such behavior was not observed during the addition of **A**, suggesting that no nanoscale aggregation occurred.

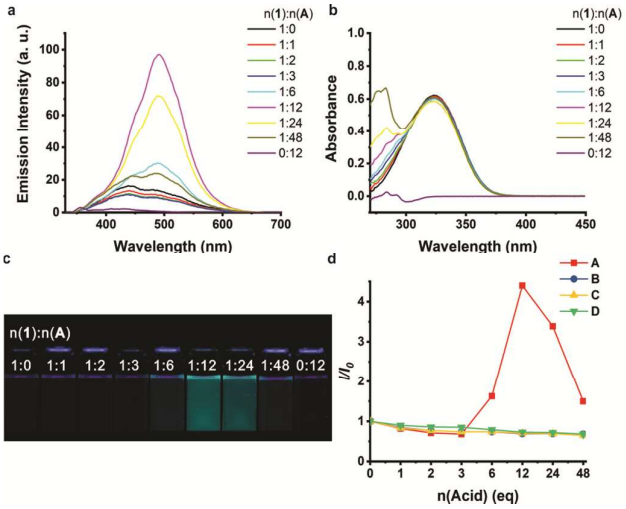

Figure 1. The emission (**a**, λ_{exc} = 320 nm) and adsorption (**b**) spectra, and digital photographs under UV irradiation (**c**, λ_{exc} = 365 nm) of **1** (10 μM, 1 eq) with different added eq of **A** in DMF solution. **d**: The relation between relative emission intensity I/I_0 and acid amount for **A**–**D**, where I is the integrated emission intensity from 330 to 700 nm.

For **A**'s isomers **B** and **C**, and the monocarboxylic benzoic acid (**D**), the I/I_0 decreased continuously to 0.68, 0.65, and 0.68, respectively, when increasing the amount of **B**–**D** from 0 to 48 eq. Compared with the results obtained for **A**, there was no significant bathochromic or hypochromic shift of the λ_{ems} values, which varied within a narrow 439±6 nm range. The λ_{abs} values almost did not change with the addition of **B**–**D**, varying between 323 and 325 nm. The corresponding spectra and data were shown in Figures S1–S3 and Table S1. Why does **A** turn ON the fluorescence of **1** while the structurally closely related **B**, **C**, and **D** do not? We performed a series of experiments to answer this question.

The ^{1}H and ^{19}F NMR titration of **1** with **A**–**D** were carried out to explore the interaction between these acids and **1**. To exclude the possibility of analyte-induced aggregation, we first added D_2O—a poor solvent for **1**, known to cause its aggregation[22b]—into the solution of **1** in DMSO-d_6. Both ^{1}H and ^{19}F NMR signals disappeared after 50% (by volume) of D_2O was added (Figure S10). No similar changes occurred in the ^{19}F NMR spectra when **A**–**D** were added (Figure S6–S9). This result also suggested that the turn ON of **1**'s fluorescence by **A** was not a result of aggregation. The ^{1}H NMR spectrum showed that the protons H^a and H^b (see Scheme 1) in **1**, which appeared at 8.40 and 8.04 ppm in the DMSO-d_6, started to merge into one signal at 8.22 ppm when 2–3 eq of **A**–**C** (Figures S6–S8) or 6 eq of **D** (Figure S9) were added. These results suggest protonation of the pyrazole nitrogens on the three branches of **1**, consistent with the lower pK_{a1} values of **A**–**C** (2.9, 3.7, and 3.5, respectively) and the higher pK_a of monoacid **D** (4.2).[27]

This journal is © The Royal Society of Chemistry 20xx

Please do not adjust margins

As would be expected, the ^{1}H NMR spectroscopic response of **1** to **A**–**D** was largely analogous. In light of this observation, we next probed whether **1** is able to recognize **A** in a mixture with its isomers or with the monocarboxylic acid **D**. To do so, we added 12 eq of **A** and 12 eq of **B**, **C**, or **D** into a DMF solution of **1**. The results in Figure 2a show that the fluorescence response of **1** (I/I_0) still increased to 1.56, 1.46,

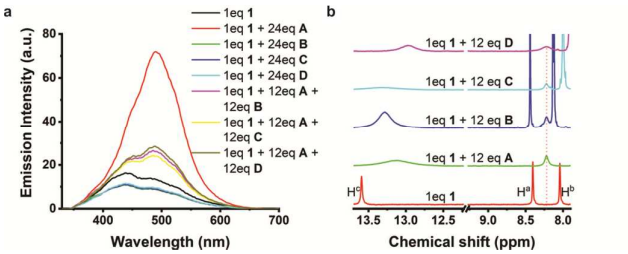

Figure 2. The emission spectra of **1** (10 μM, 1 eq) mixed with one or two aromatic acids in 24 eq (**a**). The influence of 12 eq aromatic acid on the ^{1}H NMR of **1** (1 eq, 1.62 mM) in DMSO-d_6 (**b**).

and 1.62 with the λ_{ems} shifting bathochromically to 486–489 nm for the mixture of **A** with **B**, **C**, and **D**, respectively. However, if only 24 eq **B**, **C**, or **D** were added to the solution of **1** in DMF, the fluorescence was quenched with I/I_0 being 0.69, 0.69, and 0.72, respectively, and the λ_{ems} changed negligibly. The I/I_0 values of the samples with the mixture of 12 eq of **A** and 12 eq of an another aromatic acid were significantly smaller than that of the sample with 24 eq of **A** alone (I/I_0 = 3.39), which suggested a competition between **A** and another aromatic acid, as all the acids were able to protonate **1** (Figure 2b). Although the fluorescence intensity increased to a smaller degree in the mixture of acids, the existence of **A** still can be determined, as the increase of I/I_0 and the red shift of λ_{ems} to 484–490 nm only occurred with the addition of **A**. Thus, **1** can recognize **A** even in the mixtures with its isomers.

Diffusion-ordered NMR spectroscopy (DOSY) measurements based on ^{19}F NMR shifts showed that the average diffusion coefficients $(\bar{D})$ of the signal at −140.51 ppm in ^{19}F NMR spectra were 1.080, 1.078, 1.139, 1.091, and 1.090×10^{-10} m^2 s^{-1} as 1 eq of **1** was mixed with 0, 12, 18, 24, and 48 eq of **A**, respectively.[28] This set of values implies that the hydrodynamic radius of the solute changed only within 5.2% after **A** was added into the solution of **1** in DMSO-d_6, excluding the aggregation after the addition of **A** (Figure S13).

DOSY NMR analysis, together with the models based **1**'s single crystal structure and optimized complexes between **1** and **A**, implies the existence of *J*- and *H*-stacking dimers and monomer of **1** in the DMSO-d_6 solution, and the existence of complexes **2**, **3**, **4**, and **5** during the titration with **A** (see ESI). A possible mechanism for the turn ON of the fluorescence of **1** with the addition of **A** is presented in Scheme 2. The addition of **A** (0–3 eq) first caused the formation of some of the relatively flexible (and therefore nonemissive) complex **3**; simultaneous decomposition of *H*- or *J*-stacking dimers to **2** resulted in the quenching the fluorescence. The increase in the amount of **A** from 3 to 12 eq caused more of complexes **3**, **4**, and **5** to be formed, and the turning ON of the fluorescence, as rigidified complexes **4** and **5** restricted intramolecular rotation of **1**. With even further increases in the amount of **A** (12–48

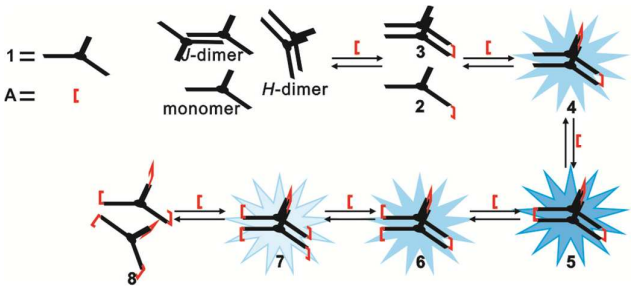

Scheme 2. A possible mechanism explaining the turn ON and OFF of the fluorescence of **1** upon exposure to increasing concentrations of **A**.

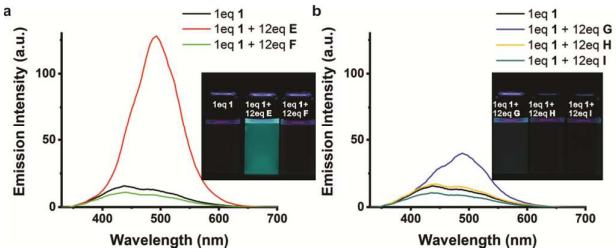

Figure 3. The emission spectra (λ_{exc} = 320 nm) of **1** (10 μM, 1 eq) with 12 eq of isomers **E** and **F** (**a**) and 12 eq aliphatic dicarboxylic acid **G**, **H**, and **I** (**b**). Insert: digital photograph under UV irradiation (λ_{exc} = 365 nm) of **1** (10 μM, 1 eq) with 12 eq of **E** and **F** (left), and **G**, **H**, and **I** (right).

eq), each pyrazolium group of **1** can complex with its own dicarboxylate, decomposing the rotation-restricted complexes **4** and **5** into flexible **6**–**8**, resulting again in the decrease of fluorescence intensity.

All the monocarboxylic acids, including **D**, and **J**–**M** quenched the fluorescence of **1** (Figure S4), which means that these monocarboxylic acids could not effectively bring two molecules of **1** into the close proximity and restrict their rotation. The key factor of this mechanism is the formation of fluorescent species like **3**–**5**. If this mechanism is reasonable, maleic acid (**E**), with two carboxyl groups in a *cis*-form sterically reminiscent of **A**, should exert similar influence over the fluorescence of **1**. To test this hypothesis, the emission spectra of **1** (1 eq) with 12 eq of **E** or its *trans*-isomer (**F**) were collected. As shown in Figure 3a, the addition of **E** caused visible aquamarine fluorescence turn ON with I/I_0 = 5.77 and bathochromic shift of λ_{ems} to 493 nm. However, the *trans*-form **F** quenched fluorescence to I/I_0 = 0.71, and the λ_{ems} almost did not change compared with the signal of **1**. The *cis*-form isomer promoted the two molecules of **1** stacking together, which restricted the intramolecular rotation and induced fluorescence. The *trans*-isomer could not form such stacks, the rotation of **1** remained flexible, and its fluorescence was quenched. This structural argument was supported by the computationally optimized structures (Figure S14). The emission spectra of **1** mixed with 12 eq of aliphatic dicarboxylic acids **G**, **H**, and **I**, show the fluorescence intensity decreasing with the lengthening distance between the COOH groups, with I/I_0 values of 2.12, 1.13, and 0.70, respectively. The addition of **G**—the shortest among the aliphatic diacids—also caused the bathochromic shift of λ_{ems} to 489 nm (Figure 3b). This observation was consistent with the purported fluorescent species proposed in the mechanism in Scheme 2, as the shorter distance between two molecules of **1**, controlled by

Please do not adjust margins

the separation between the COOH groups of aliphatic dicarboxylic acid, restricts the intramolecular rotation more effectively and results in a stronger fluorescence turn ON.

In conclusion, AIEgen **1** can be used as a fluorescent sensor to selectively recognize dicarboxylic acids with closely positioned COOH groups (including **A**, **E**, and **M**) from their isomers or homologs. Two molecules of **1** held together by dicarboxylic acids are likely responsible for the turning ON of the fluorescence, as they restrict each other's intramolecular rotation. Such fluorescence phenomena—observed in dilute solution—may present a complementary approach to the use of AIE in solutions approaching aggregate formation in the sensing of practically relevant analytes.

We acknowledge the financial support from the National Science Foundation (award DMR-1507664) and the Welch Foundation (award E-1768). O. Š. M. is a Cottrell Scholar of the Research Corporation for Science Advancement.

Notes and references

1 N. Raimundo, B. E. Baysal, G. S. Shadel, *Trends Mol. Med.*, 2011, **17**, 641–649.
2 T. Hagen, M. S. Korson, M. Sakamoto, J. E. Evans, *Clin. Chim. Acta*, 1999, **283**, 77–88.
3 https://gimasterycourse.com/wp-content/uploads/Clinical-Significance-of-the-OAT.pdf
4 T. A. M. Msagati, *Chemistry of Food Additives and Preservatives*, Wiley, 2012, pp. 125–130.
5 (*a*) Z. J. Li, Y. Abramov, J. Bordner, J. Leonard, A. Medek, A. V. Trask, *J. Am. Chem. Soc.*, 2006, **128**, 8199–8210; (*b*) P. Sanphui, S. Tothadi, S. Ganguly, G. R. Desiraju, *Mol. Pharm.*, 2013, **10**, 4687–4697.
6 (*a*) A. Díaz, R. Katsarava, J. Puiggalí, *Int. J. Mol. Sci.*, 2014, **15**, 7064–7123; (*b*) G. P. Karayannidis, D. S. Achilias, *Macromol. Mater. Eng.*, 2007, **292**, 128–146.
7 (*a*) A. M. Booth, D. O. Topping, G. McFiggans, C. J. Percival, *Phys. Chem. Chem. Phys.*, 2009, **11**, 8021–8028; (*b*) B. Zobrist, C. Marcolli, T. Koop, B. P. Luo, D. M. Murphy, U. Lohmann, A. A. Zardini, U. K. Krieger, T. Corti, D. J. Cziczo, S. Fueglistaler, P. K. Hudson, D. S. Thomson, T. Peter, *Atmos. Chem. Phys.*, 2006, **6**, 3115–3129.
8 (*a*) D. Curiel, M. Más-Montoya, G. Sánchez, *Coord. Chem. Rev.*, 2015, **284**, 19–66; (*b*) R. J. Fitzmaurice, G. M. Kyne, D. Douheret, J. D. Kilburn, *J. Chem. Soc., Perkin Trans. 1*, 2002, 841–864.
9 (*a*) Z. Liu, S. K. M. Nalluri, J. F. Stoddart, *Chem. Soc. Rev.*, 2017, **46**, 2459–2478; (*b*) N. H. Evans, P. D. Beer, *Angew. Chem. Int. Ed.*, 2014, **53**, 11716–11754.
10 (*a*) V. Kumar, T. Pilati, G. Terraneo, G. Ciancaleoni, A. Macchioni, G. Resnati, P. Metrangolo, *Angew. Chem. Int. Ed.*, 2018, **57**, 1327–1331; (*b*) I. L. Karle, D. Ranganathan, V. Haridas, *J. Am. Chem. Soc.*, 1997, **119**, 2777–2783.
11 T. Kusukawa, K. Inoue, H. Obata, R. Mura, *Tetrahedron*, 2017, **73**, 661–670.
12 H.-T. Feng, J.-B. Xiong, J. Luo, W.-F. Feng, D. Yang, Y.-S. Zheng, *Chem. Eur. J.*, 2017, **23**, 644–651.
13 (*a*) F. Garcia-Tellado, S. J. Geib, S. Goswami, A. D. Hamilton, *J. Am. Chem. Soc.*, 1991, **113**, 9265–9269; (*b*) J. Yang, E. Fan, S. J. Geib, A. D. Hamilton, *J. Am. Chem. Soc.*, 1993, **115**, 5314–5315.
14 (*a*) J. Zhao, T. M. Fyles, T. D. James, *Angew. Chem. Int. Ed.*, 2004, **43**, 3461–3464; (*b*) J. Zhao, T. D. James, *Chem. Commun.*, 2005, 1889–1891.
15 (*a*) J. Y. C. Lim, I. Marques, V. Félix, P. D. Beer, *Angew. Chem. Int. Ed.*, 2018, **57**, 584–588; (*b*) M. Denis, S. M. Goldup, *Angew. Chem. Int. Ed.*, 2018, **57**, 4462–4464.
16 (*a*) J. Frey, C. Tock, J.-P. Collin, V. Heitz, J.-P. Sauvage, *J. Am. Chem. Soc.*, 2008, **130**, 4592–4593; (*b*) J.-P. Collin, J. Frey, V. Heitz, J.-P. Sauvage, C. Tock, L. Allouche, *J. Am. Chem. Soc.*, 2009, **131**, 5609–5620; (*c*) J.-P. Collin, F. Durola, V. Heitz, F. Reviriego, J.-P. Sauvage, Y. Trolez, *Angew. Chem. Int. Ed.*, 2010, **49**, 10172–10175.
17 (*a*) S. Samanta, C. Kar, G. Das, *Anal. Chem.*, 2015, **87**, 9002–9008; (*b*) F. Sancenón, R. Martínez-Máñez, M. A. Miranda, M.-J. Seguí, J. Soto, *Angew. Chem. Int. Ed.*, 2003, **42**, 647–650; (*c*) U. R. G., R. Lo, S. Roy, T. Banerjee, B. Ganguly, A. Das, *Chem. Commun.*, 2013, **49**, 9818–9820.
18 J. Luo, Z. Xie, J. W. Y. Lam, L. Cheng, H. Chen, C. Qiu, H. S. Kwok, X. Zhan, Y. Liu, D. Zhu, B. Z. Tang, *Chem. Commun.*, 2001, 1740–1741.
19 (*a*) J. Mei, N. L. C. Leung, R. T. K. Kwok, J. W. Y. Lam, B. Z. Tang, *Chem. Rev.*, 2015, **115**, 11718–11940; (*b*) J. Mei, Y. Hong, J. W. Y. Lam, A. Qin, Y. Tang, B. Z. Tang, *Adv. Mater.*, 2014, **26**, 5429–5479; (*c*) Y. Hong, J. W. Y. Lam, B. Z. Tang, *Chem. Soc. Rev.*, 2011, **40**, 5361–5388; d) Y. Hong, J. W. Y. Lam, B. Z. Tang, *Chem. Commun.*, 2009, 4332–4353.
20 (*a*) N. Sinha, L. Stegemann, T. T. Y. Tan, N. L. Doltsinis, C. A. Strassert, F. E. Hahn, *Angew. Chem. Int. Ed.*, 2017, **56**, 2785–2789; (*b*) X. Yan, T. R. Cook, P. Wang, F. Huang, P. J. Stang, *Nat. Chem.*, 2015, **7**, 342–348; (*c*) T. Noguchi, B. Roy, D. Yoshihara, Y. Tsuchiya, T. Yamamoto, S. Shinkai, *Chem. Eur. J.*, 2014, **20**, 381–384; (*d*) J. Zhao, D. Yang, Y. Zhao, X.-J. Yang, Y.-Y Wang, B. Wu, *Angew. Chem. Int. Ed.*, 2014, **53**, 6632–6636.
21 Y. Liu, C. Deng, L. Tang, A. Qin, R. Hu, J. Z. Sun, B. Z. Tang, *J. Am. Chem. Soc.*, 2011, **133**, 660–663.
22 (*a*) T.-H. Chen, I. Popov, W. Kaveevivitchai, Y.-S. Chuang, Y. Chen, O. Daugulis, A. J. Jacobson, O. Š. Miljanić, *Nat. Commun.*, 2014, **5**, 14096–14098; (*b*) Z. Zhang, M. I. Hashim, O. Š. Miljanić, *Chem. Commun.*, 2017, **53**, 10022–10025; (*c*) M. I. Hashim, H. T. M. Le, T.-H. Chen, Y.-S. Chen, O. Daugulis, C.-W. Hsu, A. J. Jacobson, W. Kaveevivitchai, X. Liang, T. Makarenko, O. Š. Miljanić, I. Popovs, H. V. Tran, X. Wang, C.-H. Wu, J. I. Wu, *J. Am. Chem. Soc.*, 2018, **140**, 6014–6026.
23 T.-H. Chen, W. Kaveevivitchai, A. J. Jacobson and O. Š. Miljanić, *Chem. Commun.*, 2015, **51**, 14096-14098.
24 C. H. Hendon, K. E. Wittering, T.-H Chen, W. Kaveevivitchai, I. Popov, K. T. Butler, C. C. Wilson, D. L. Cruickshank, O. Š. Miljanić, A. Walsh, *Nano Lett.*, 2015, **15**, 2149–2154.
25 (*a*) C. López, R. M. Claramunt, M. Á. García, E. Pinilla, M. R. Torres, I. Alkorta, J. Elguero, *Cryst. Growth Des.*, 2007, **7**, 1176–1184; (*b*) T. Basu, H. A. Sparkes, R. Mondal, *Cryst. Growth Des.*, 2009, **9**, 5164–5175.
26 (*a*) S. Xie, A. Y. H. Wong, R. T. K. Kwok, Y. Li, H. Su, J. W. Y. Lam, S. Chen, B. Z. Tang, *Angew. Chem. Int. Ed.*, 2018, **57**, 5750–5753; (*b*) Y. Chen, W. Zhang, Z. Zhao, Y. Cai, J. Gong, R. T. K. Kwok, J. W. Y. Lam, H. H. Y. Sung, I. D. Williams, B. Z. Tang, *Angew. Chem. Int. Ed.*, 2018, **57**, 5011–5015; (*c*) B. Xu, J. He, Y. Dong, F. Chen, W. Yu and W. Tian, *Chem. Commun.*, 2011, **47**, 6602–6604; (*d*) Z. Chen, J. Zhang, M. Song, J. Yin, G. Yu and S. H. Liu, *Chem. Commun.*, 2015, **51**, 326–329.
27 J. R. Rumble, ed., CRC Handbook of Chemistry and Physics, 98th Edition (Internet Version 2018), CRC Press/Taylor & Francis, Boca Raton, FL.
28 It should be noted that DOSY NMR and fluorescence spectroscopies operate in very different concentration regimes, and may not model the behaviour of same species. However, together they paint a consistent picture of emission not being caused by aggregation. See also: B. M. Schulze, D. L. Watkins, J. Zhang, I. Ghiviriga, R. K. Castellano, *Org. Biomol. Chem.*, 2014, **12**, 7932–7936.

This journal is © The Royal Society of Chemistry 20xx

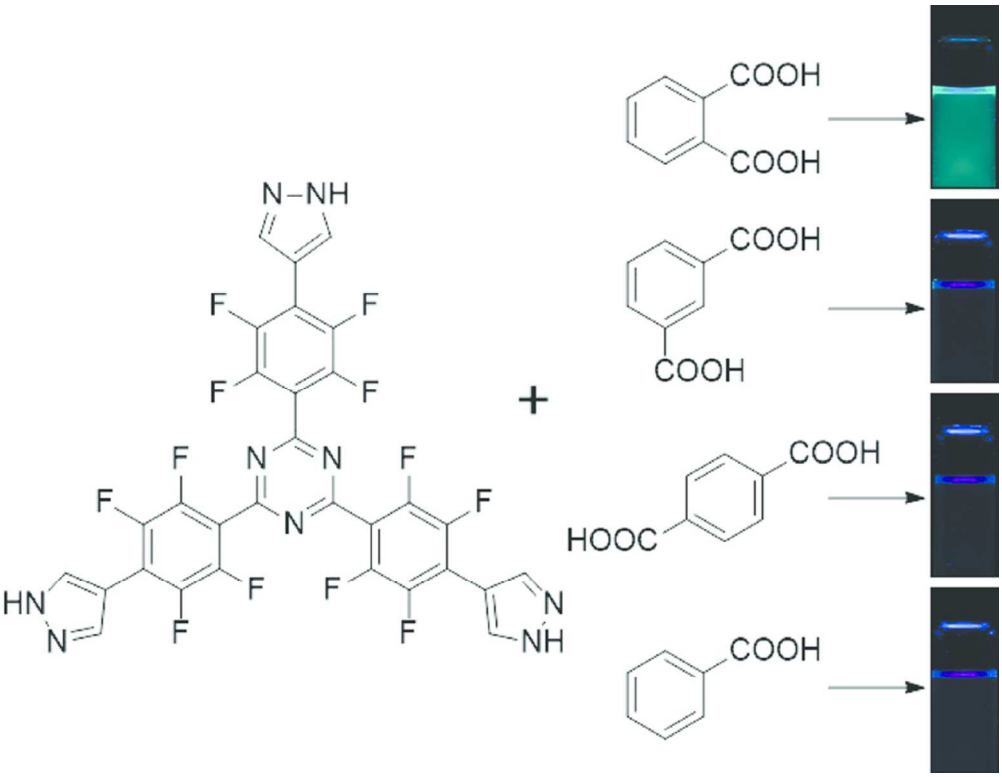

76x58mm (300 x 300 DPI)